GIScience & Remote Sensing

ISSN: (Print) (Online) Journal homepage: www.tandfonline.com/journals/tgrs20

Methods to compare sites concerning a category's change during various time intervals

Thomas Mumuni Bilintoh, Robert Gilmore Pontius Jr & Aiyin Zhang

To cite this article: Thomas Mumuni Bilintoh, Robert Gilmore Pontius Jr & Aiyin Zhang (2024) Methods to compare sites concerning a category's change during various time intervals, GIScience & Remote Sensing, 61:1, 2409484, DOI: 10.1080/15481603.2024.2409484

To link to this article: https://doi.org/10.1080/15481603.2024.2409484

Published online: 20 Oct 2024.

GISCIENCE & REMOTE SENSING
2024, VOL. 61, NO. 1, 2409484
https://doi.org/10.1080/15481603.2024.2409484

Taylor & Francis
Taylor & Francis Group

Methods to compare sites concerning a category's change during various time intervals

Thomas Mumuni Bilintoh, Robert Gilmore Pontius Jr and Aiyin Zhang

School of Geography, Clark University, Worcester, USA

ABSTRACT

This paper presents new methods to analyze a category's change through a time series of maps, even when the time intervals have inconsistent durations. The methods include an option to facilitate comparison among sites by expressing results as an annual percentage of each site's unified size. A site's unified size is the union of where the category exists at any of the site's time points. The methods also specify gross losses, gross gains, eight trajectories, and three components: Quantity, Exchange, and Alternation. The illustrative application compares maps of the marsh category for three Long-Term Ecological Research sites: Plum Island Ecosystems (PIE), Georgia Coastal Ecosystems (GCE), and the Virginia Coast Reserve (VCR). The application analyzes marsh's changes during two time intervals that have unequal durations within each site's distinct temporal extent. Results show that PIE has the fastest change during each site's temporal extent. Gross change is more than double the quantity change for all sites. Exchange accounts for most of the change in GCE, while Alternation accounts for most of the change in PIE and VCR. The methods provide more information than popular methods that quantify annual net change. Our *timeseriesTrajectories* R package performs the analysis and is available for free at https://github.com/bilintoh/timeseriesTrajectories.

ARTICLE HISTORY
Received 14 March 2024
Accepted 23 September 2024

KEYWORDS
Alternation; land change; time series; Marsh; Trajectories

1. Introduction

Quantifying land change is critical for understanding human society, climate change, and food security (Chowdhury et al. 2017; Feng and Tong 2018; Grekousis, Mountrakis, and Kavouras 2016; Molotoks, Smith, and Dawson 2021). Researchers want to analyze land change, such as deforestation, reforestation, afforestation, agricultural shift, and land alteration due to climate change (Borrelli et al. 2020; Clement and Amezaga 2008; Heintzman et al. 2024; Ruskule et al. 2012; Zomer et al. 2008). Researchers and organizations such as the Food and Agriculture Organization, United Nations, and Intergovernmental Panel on Climate Change have advocated for research to facilitate site comparison regarding land cover categories such as water, forest, urban, and cropland (Dasgupta et al. 2009; FAO and JRC 2012; Taubert et al. 2018). New methods are necessary to analyze a category's change across multiple sites and time intervals to reveal important information concerning a category's behavior within and among sites because popular methods have several deficiencies. Our manuscript answers this call by introducing a method to alleviate the deficiencies in existing methods that scientists tend to use.

Furthermore, existing methods frequently use equations to compare land change that are inappropriate or challenging to interpret. A popular approach to compare a category's change across sequential time intervals and sites is to express annual net change as a percentage that relies on both the start size during each time interval and the duration of the time interval (Pontius, Huang, et al. 2017). Three equations are popular and distinct, while authors sometimes fail to report the equations that they use. One equation to compute annual percent net change portrays linear change, while other equations portray exponential change with base e or $(1+p)$, where p is the annual proportional net change during a time interval. The two exponential equations give the same mathematical relationship but the numerical value of the annual percentage that derives from the equation with base e differs from the numerical value of the annual percentage that derives from the equation

CONTACT Thomas Mumuni Bilintoh tbilintoh@clarku.edu

with base (1+p). The literature includes examples of these equations and publications that report annual percent net change while not giving the equation (Burns, Alber, and Alexander 2021; Liu et al. 2003; Puyravaud 2003).

These three popular equations have drawbacks, making them inappropriate, unnecessarily complicated, or challenging to interpret for various reasons. First, each equation includes both the start size of each time interval and the duration of the time interval, so if both factors vary across consecutive time intervals, then interpretation can be confusing because the variation in the annual percentage across sequential time intervals is due to variation in the start size and the duration. Second, even if the duration is constant across consecutive time intervals, each time interval in a series can have a distinct start size, so the annual percent net change from the start of each consecutive interval can vary even when the absolute size of net change is identical across sequential time intervals. Third, all the equations produce undefined results when a category grows from zero, but many phenomena can grow from zero, such as the gain of a newly introduced crop or the gain of built land around a newly created road. Fourth, the exponential equation with base e generates undefined results when a category decays to zero, while the other two equations compute a 100% decrease during the time interval. Fifth, the three popular equations can be confusing when comparing across sites when the sizes of the sites vary and when the prevalence of the category within the site varies through time. Authors should use and explain an equation that is easily interpretable across multiple time intervals and across multiple sites.

Some existing methods reveal how a category's gross losses and gross gains form components of difference. Pontius and Millones (2011) showed how gross loss and gross gain combine to form two components: Quantity and Allocation. Pontius and Santacruz (2014) showed how to quantify the changes of a categorical variable across time intervals of varying duration using three components: Quantity, Exchange, and Shift. Aldwaik and Pontius (2012) introduced Intensity Analysis, which expresses category-level annual gross losses and annual gross gains across time intervals of varying duration. However, those approaches miss important insights concerning a location's trajectory through sequential time intervals because those methods fail to track individual locations through the time series. Our new method builds on the methods of Pontius, Krithivasan, et al. (2017), who gave methods to track individual pixels through a time series as opposed to the traditional methods of analyzing each time interval independently of the other time intervals. Winkler et al. (2021) quantified the global gross gains and gross losses of forest, cropland, and pasture through a time series. Their map of change has a legend entry called "Gain and Loss" to denote locations that experienced more than one change during the time series. Our methods offer additional details and are appropriate to analyze data of the format of Winkler et al. (2021).

We address the drawbacks of the popular methods by creating the concept of the unified size, which is the union of observations that have presence of the category at any time point. The unified size is constant across all time intervals, while we account for the duration of each time interval. The unified size is the relevant subset of the site's extent. For example, a raster GIS database's extent is frequently an arbitrary polygon that bounds the category of interest. If the data derive from remote sensing, then the bounds of the remotely sensed image dictate an arbitrary region. Various arbitrary regions can contain the category of interest. Some authors might be tempted to report change as a percentage of the rectangular region or of the region that was remotely sensed, which can contain many pixels that are irrelevant because the pixels show absence of the category at all time points. It is confusing when authors report the change as a percentage of an arbitrary region of the database's spatial extent. Readers need to know the size of change with respect to a relevant constant region, which the unified size is. Therefore, our methods facilitate comparison among sites that vary in the prevalence of the category, the durations of time intervals, and the duration of temporal extents.

Additionally, our manuscript presents new methods to compare sites by specifying gross losses, gross gains, eight trajectories, and three components: Quantity, Exchange, and Alternation. The results give insights into the speed of gross loss, speed of gross gain, speed of net change, acceleration of change, and reversal of change. The methods apply to many professions, particularly Remote Sensing and Land Change Science.

Subsection 2.1 shows the maps of land change for three sites, while subsection 2.2 gives simplified data to illustrate the equations. Section 3 gives the results for the data in subsection 2.1. Section 4 discusses the results and concepts. Section 5 concludes by inviting readers to use the free package in the software R.

2. Data and methods

2.1. Data and study area

The data are raster land cover maps for three sites within the United States Long-Term Ecological Research Network (LTER) funded by the National Science Foundation (Burns, 2020). Our methods

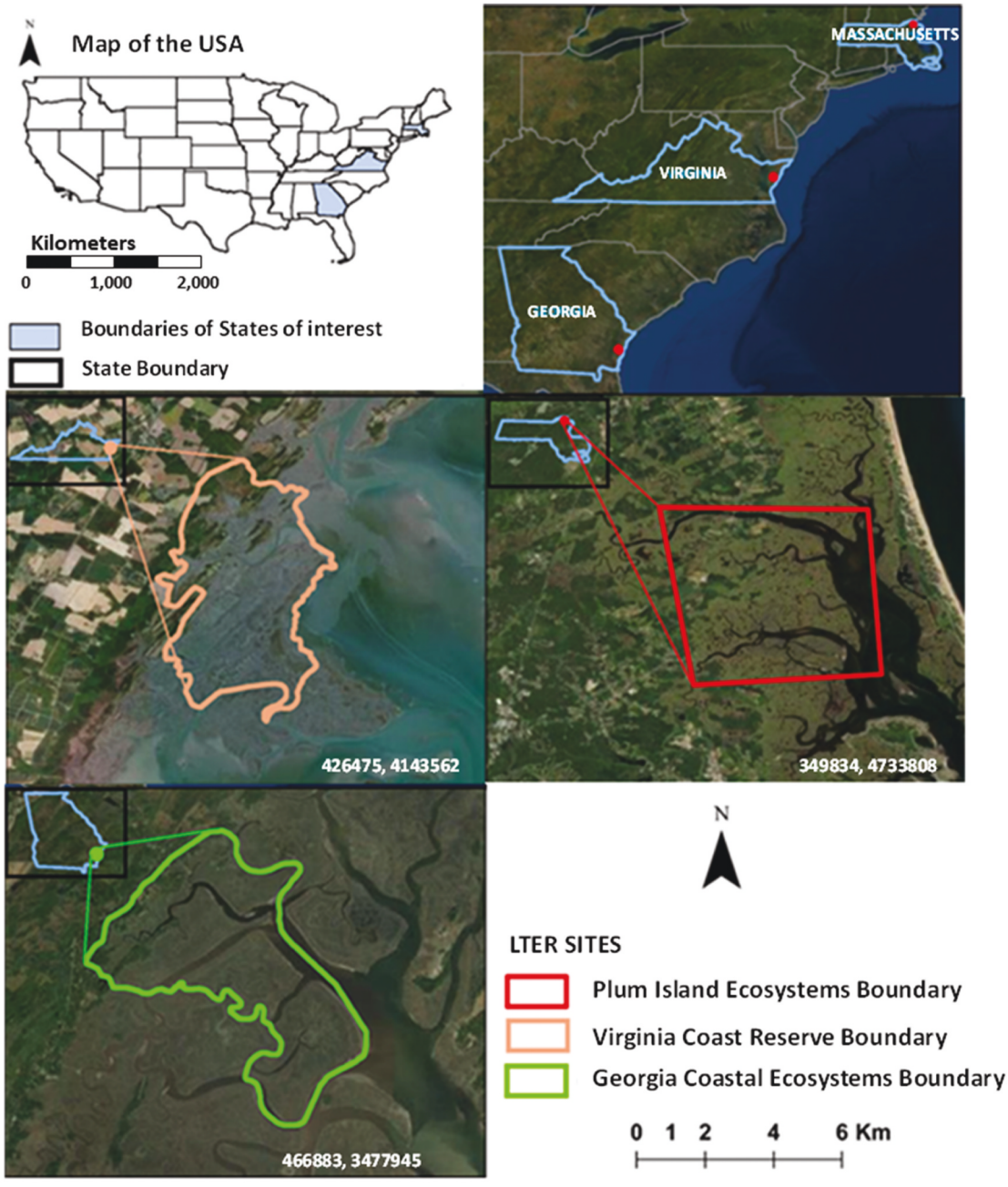

Figure 1. The location of the three LTER sites: PIE, GCE, and VCR. The maps are in the US 83 UTM zone 18 projection. Thus, the coordinates in the lower right corners show the center coordinates of each site in meters.

Table 1. Description of data for each LTER site. The error as a percent of the extent derives from pixel resolution, georectification, and digitization (Burns, Alber, and Alexander 2021).

LTER Site	Acquisition Date	Image	Image Scale	Error (%)
PIE	1Nov 1938	Black and white	1:25,000	4
	11 June 1971	Black and white	1:20,000	5
	April 2013	Orthomosaic	-	2
GCE	28 November 1942	Black and white	1:40,000	4
	2 December 1972	Color aerial photograph	1:20,000	3
	Early 2013	Orthomosaic	-	3
VCR	2 February 1949	Black and white	1:20,000	2
	20 October 1957	Black and white	1:20,000	3
	Spring 2013	Orthomosaic	-	3

apply to raster GIS files and tabular data, while the LTER data sets are available in raster and vector GIS formats; thus, we analyze the raster GIS files for the three LTER sites. Figure 1 shows the three sites: Plum Island Ecosystems (PIE), Georgia Coastal Ecosystems (GCE), and Virginia Coast Reserve (VCR). Table 1 provides information about the date of acquisition, scale, and quality associated with each land cover map. Burns, Alber, and Alexander (2021) describe how LTER scientists created the land cover maps.

Our manuscript analyzes the marsh category in raster maps that have a spatial resolution of 10-by-10 m. Figure 2 shows an overlay of binary maps where 0 denotes the absence of marsh, and 1 denotes the presence of marsh.

Marshes in the three LTER sites provide several ecosystem services, including storm protection, habitat provision, nutrient cycling, and carbon storage (Roy, Byrnes, and Mavrommati 2024). Rising sea level influences these ecosystem services. For example, sea-level rise could cause cordgrass to become flooded, thus causing cordgrass to shift to higher elevations. Measuring and visualizing these changes are crucial for understanding the relationship between changes and the ecosystem function. Thus, scientists need methods that compare marsh change across the three sites. Our manuscript proposes a generalized method that compares sites concerning any particular category's changes across various time intervals.

2.2. Methods

The *timeseriesTrajectories* package in R creates for each site 1) a map that shows the trajectories of the category, 2) a stacked bar graph that shows gross loss and gross gain during each time interval, and 3) a stacked bar graph that shows three components of change during the temporal extent.

The *timeseriesTrajectories* package reads raster or tabular data that show the category's presence or absence for each observation at each time point. Figure 3 gives example data to describe the trajectory patterns. The example data show 12 observations at 5 time points. The first column identifies 12 observations. The second column specifies each observation's trajectory during the time series. The next five columns give either 0 for the absence or 1 for the presence of the binary variable at time points $t = 0, 1, 2, 3, 4$. For example, ID observation 4 is trajectory 2, which derives from a time series with Y values 0, 0, 1, 1, and 1 corresponding to time points 2000, 2001, 2002, 2003, and 2005. We designed the method to work when the variable is any non-negative number, for which a simple case is where the variable is 0 for absence and 1 for presence. The number below each t is the year; thus, the first three time intervals have a duration of 1 year, and the fourth time interval has a duration of 2 years. Table 2 defines the trajectories. Trajectories 1 and 2 each have exactly one change during the time series. Alternation is a pair of loss and gain at a location during the time series. Trajectories 3 and 4 have an odd number of changes greater than one, while trajectories 5 and 6 have an even number of changes greater than zero, thus trajectories 3–-6 have Alternation. Trajectories 7 and 8 have zero changes.

The definitions in Table 2 and the equations use the notation in Table 3. The unified size is a new concept that facilitates comparison among sites and across time intervals. The unified size is the union of the locations where the category exists at any time point. The research question of a particular case

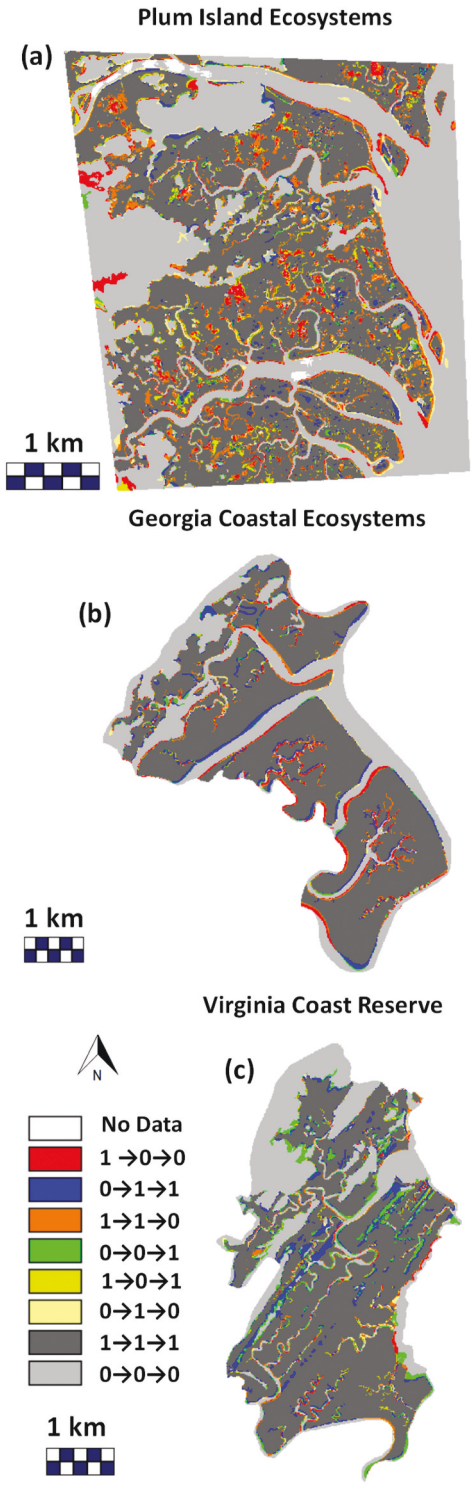

Figure 2. (a) Plum Island ecosystems, (b) Georgia ecosystems, and (c) Virginia coast Reserve's overlaid binary maps. The → symbol shows the flow through time where 0 means marsh's absence and 1 means the marsh's presence.

study dictates the selection of *U*, which the user must specify. Equation 1 gives the three options to define *U*, which is a factor in the denominator of equations 2, 3, 7 and 8. The first option is $U = 1$, in

ID	Trajectory	Y *t=0* 2000	Y *t=1* 2001	Y *t=2* 2002	Y *t=3* 2003	Y *t=4* 2005
1	1	1	0	0	0	0
2	1	1	1	0	0	0
3	1	1	1	1	0	0
4	2	0	0	1	1	1
5	2	0	0	0	1	1
6	3	1	1	0	1	0
7	4	0	1	0	1	1
8	5	1	1	0	1	1
9	6	0	1	0	1	0
10	7	1	1	1	1	1
11	8	0	0	0	0	0
12	0	na	0	0	0	0

Figure 3. Example data illustrates a binary variable's trajectories during a time series. 0 denotes absence, while 1 denotes the presence of the category.

which case the results are in annual units of *Y*. The second option is *U*=*E*, where the user sets *E* so the results are in an annual proportion of *E*. The third option computes the results as a proportion of the unified size where the double summation in equation 1 computes the unified size. We recommend scientists use the unified size when comparing across sites to avoid a variety of problems that our manuscript's Introduction explains.

Equation 2 computes a negative number to indicate an annual loss for a particular trajectory during each time interval as a proportion of *U*. Equation 3 computes a positive number to indicate annual gain for a particular trajectory during each time interval as a proportion of *U*. Equations 2 and 3 have the duration of the time interval in the denominator to annualize the results, which is necessary to account for the possibility that the durations of the time intervals vary for a single site or that the durations of the temporal extents vary among sites. Equation 4 computes a negative number for gross loss during the site's temporal extent by summing across trajectories where each time interval is weighted by its duration. Similarly, equation 5 computes a positive number for

Table 2. Description of the trajectories where Y_{jmt} is the value of variable Y in trajectory j of cell m at time t.

Code	Trajectory	Color	Definition
0	Mask	White	Eliminated from computation
1	Loss without Alternation	Dark Red	$Y_{1m0} > Y_{1mT}$ and $Y_{1mt-1} \geq Y_{1mt}$ for all t
2	Gain without Alternation	Dark Blue	$Y_{2m0} < Y_{2mT}$ and $Y_{2mt-1} \leq Y_{2mt}$ for all t
3	Loss with Alternation	Light Red	$Y_{3m0} > Y_{3mT}$ and $Y_{3mt-1} < Y_{3mt}$ for at least one t
4	Gain with Alternation	Light Blue	$Y_{4m0} < Y_{4mT}$ and $Y_{4mt-1} > Y_{4mt}$ for at least one t
5	All Alternation Loss First	Dark Yellow	$Y_{5m0} = Y_{5mT}$ and loss is the first change
6	All Alternation Gain First	Light Yellow	$Y_{6m0} = Y_{6mT}$ and gain is the first change
7	Stable Presence	Dark Gray	$Y_{7mt-1} = Y_{7mt} > 0$ for $t = 1, 2, \ldots T$
8	Stable Absence	Light Gray	$Y_{8mt-1} = Y_{8mt} = 0$ for $t = 1, 2, \ldots T$

Table 3. Mathematical notation for equations.

Symbol	Meaning
d_t	1 or duration of time interval in years from time t-1 to t where $d_t > 0$
E	Possible value for U to customize the units of the results
G_{jt}	Annual gross gain as a proportion of the unified size in trajectory j from time t-1 to t. $G_{jt} \geq 0$
j	Index for trajectory where $j = 1, 2, 3, 4, 5, 6, 7, 8$
J	Number of trajectories in the region defined by the user = 7 or 8
L_{jt}	Annual gross gain as a proportion of the unified size in trajectory j from time t-1 to t. $L_{jt} \leq 0$
m	Index for a cell in trajectory j where $m = 1, 2, \ldots, M_j$
M_j	Number of cells in trajectory j
S_t	Size of Y at time t
t	Index for a time point where $t = 0, 1, 2, \ldots, T$
T	Number of time intervals where $T \geq 1$
U	Factor in the denominator of the results
Y_{jmt}	Value of variable Y in trajectory j of cell m at time t

the gross gain during the site's temporal extent. Equation 6 adds the gross loss and gross gain to compute net change. Equation 7 computes the quantity component as the absolute value of net change, which relies on the difference between time point 0 and the final time point T in the first four trajectories. Equation 8 computes the exchange component, which relies on the difference between time point 0 and the final time point T in the first four trajectories. Equation 9 computes the Alternation component, which relies on all time intervals. Equation 10 computes the category's size at each time point.

$$U = 1 \text{ or } E \text{ or } \sum_{j=1}^{7} \sum_{m=1}^{M_j} \text{MAXIMUM}\left(Y_{jm0}, Y_{jm1}, Y_{jm2}, \ldots Y_{jmT}\right) \quad (1)$$

$$L_{jt} = \left[\sum_{m=1}^{M_j} \text{MINIMUM}\left(0, Y_{jmt} - Y_{jmt-1}\right)\right] / \left(U d_t\right) \quad (2)$$

$$G_{jt} = \left[\sum_{m=1}^{M_j} \text{MAXIMUM}\left(0, Y_{jmt} - Y_{jmt-1}\right)\right] / \left(U d_t\right) \quad (3)$$

$$\text{Loss} = \left[\sum_{j=1}^{6} \sum_{t=1}^{T} \left(L_{jt} d_t\right)\right] / \left(\sum_{t=1}^{T} d_t\right) \quad (4)$$

$$\text{Gain} = \left[\sum_{j=1}^{6} \sum_{t=1}^{T} \left(G_{jt} d_t\right)\right] / \left(\sum_{t=1}^{T} d_t\right) \quad (5)$$

$$\text{Net} = \text{Loss} + \text{Gain} \quad (6)$$

$$\text{Quantity} = |\text{Net}| = \left|\sum_{j=1}^{4} \sum_{m=1}^{M_j} \left(Y_{jmT} - Y_{jm0}\right)\right| / \left(U \sum_{t=1}^{T} d_t\right) \quad (7)$$

$$\text{Exchange} = \left[\left(\sum_{j=1}^{4} \sum_{m=1}^{M_j} \left|Y_{jmT} - Y_{jm0}\right|\right) / \left(U \sum_{t=1}^{T} d_t\right)\right] - \text{Quantity} \quad (8)$$

$$\text{Alternation} = \text{Gain} - \text{Loss} - \text{Exchange} - \text{Quantity} \quad (9)$$

$$S_t = \sum_{j=1}^{J} \sum_{m=1}^{M_j} Y_{jmt} \quad (10)$$

Figure 4 shows stacked bars for each time interval of the example data. The vertical axis is the annual gross change as a percentage of the unified size. The gains rise above the time axis, while the losses drop below. The colors within the stacked bars indicate the trajectories. The vertical length from the top of the gain to the bottom of the loss indicates the speed of change during each time interval. The horizontal length of each stack indicates the duration of the time interval. Thus, the area of each interval's stack is the size of the change during the interval. The horizontal Gross Loss and Gross Gain lines derive from equations 4 and 5,

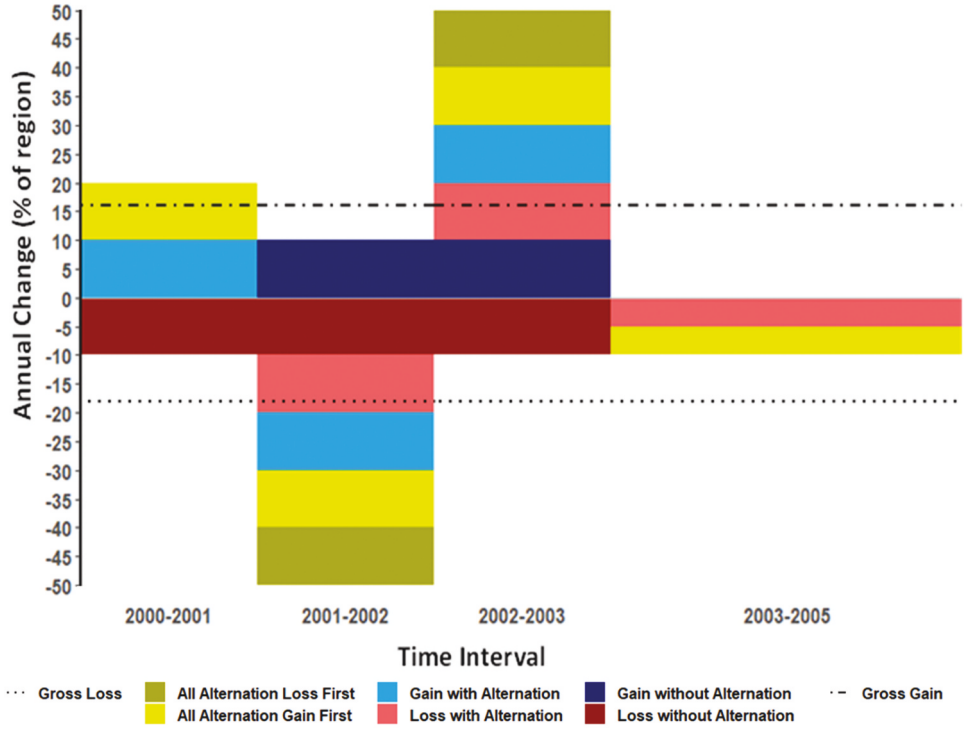

Figure 4. Stacked bars for the example data during four time intervals expressed as the annual percentage of the unified size. The fourth time interval is twice as wide as the other time intervals because the fourth time interval is two years while the other intervals are one year each.

respectively, which indicate change averaged over the temporal extent.

Figure 5 has the same vertical axis as Figure 4. Figure 5 shows the three components of Quantity, Exchange, and Alternation. The quantity component measures the absolute net change between time point 0 and time point *T*, which is the final time point of the series. The legend specifies that the quantity component derives from net loss rather than net gain. Exchange measures the simultaneous

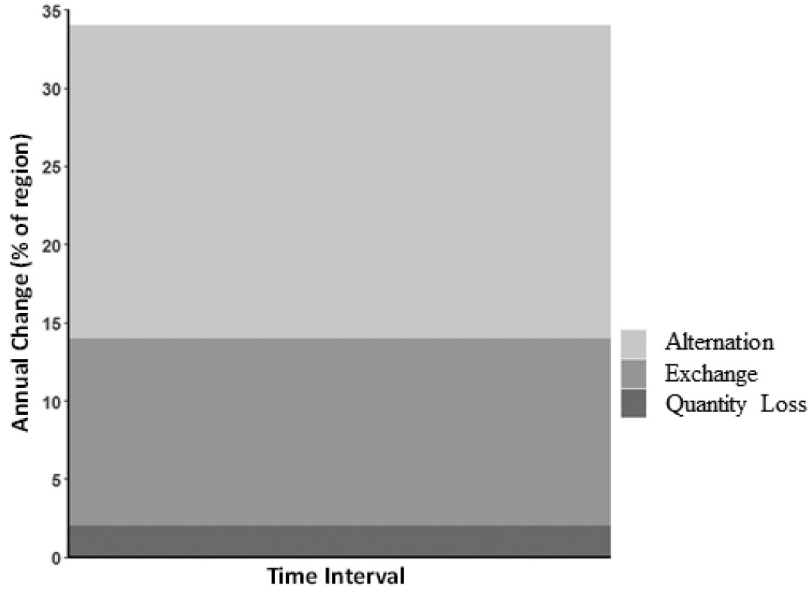

Figure 5. Three components of change during the temporal extent expressed as the annual percentage of the unified size.

gain at some locations and loss at other locations between time point 0 and the final time point of the series. Alternation measures pairs of gain and loss at an observation through the time series.

3. Results

Figure 6 shows maps of the six trajectories for the marsh category in PIE, GCE, and VCR. The number of time intervals determines the number of possible trajectories. The sites have two time intervals, hence have trajectories 1, 2, 5, 6, 7, and 8. Trajectories 3 and 4 require at least three time intervals. The maps show that change occurs nearer the edges of the patches for all three sites. The trajectory Loss without Alternation is the largest trajectory for PIE and GCE. In contrast, Gain without Alternation accounts for most of the change in VCR.

Figure 7 facilitates comparison among the sites. Figures 7a, c, and e show how the trajectories form the gross loss and gain during each time interval. Figures 7b, d, and f show how the three components form the speed of gross change during each site's temporal extent.

PIE experiences more loss than gain during each time interval; therefore, PIE's Gross Loss line is farther from the time axis than PIE's Gross Gain line, while the Quantity component derives from net loss. Alternation accounts for about half of the change during PIE's temporal extent.

In GCE, gross loss nearly equals gross gain during each time interval; therefore, GCE's Gross Loss line is nearly the same distance from the time axis as GCE's Gross Gain line, while the quantity component is nearly zero. Most of GCE's change derives from equal sizes of trajectories 1 and 2; therefore, exchange accounts for most of the change during GCE's temporal extent.

VCR experiences more gain than loss during each time interval; therefore, VCR's Gross Gain line is farther from the time axis than VCR's Gross Loss line, while the Quantity component derives from net gain. VCR's Quantity component is the largest among the three sites. Quantity, Exchange, and Alternation are distributed more equally in VCR than in the other sites.

For all three sites, the range of the stacked bars during the first time interval is greater than the vertical range of the stacked bars during the second time interval, indicating that change decelerates from the first to the second time interval. The sum of the components of change shows that the speed of change during each site's temporal extent is fastest in PIE and slowest in GCE.

4. Discussion

4.1. The implications of alternation in marsh ecosystems

Alternation requires a times series of at least two time intervals from three time points. However, many of the existing studies of change involving marsh analyzed only one time interval or analyzed each time interval independently from other time intervals during the series; thus, failing to show Alternation. For example, Campbell et al. (2022) analyzed the change in global salt marsh across four time intervals during the temporal extent of 2000–2019; however, they measured loss and gain of salt marsh at each individual time interval, missing crucial change trajectories such as Alternation. In another study, Lopes et al. (2020) gave a graph to show the size of salt mash at each of 35 years using Landsat imagery in Tagus Estuary, Portugal. The graph showed time on the horizontal axis and the size of marsh on the vertical axis in a manner that each time point derived from one image. The procedure did not analyze all the time points simultaneously. Such procedures show net change, but fail to show gross loss, gross gain, and Alternation.

Alternation accounts for most of the change in PIE. Alternation indicates a reversal of a previous change, which can have several implications for the marsh ecosystem. For example, variations in tide levels could cause a marsh loss followed by a marsh gain at the same location (Fagherazzi et al. 2020). Such change could impact the migratory patterns of organisms that use marsh vegetation as their habitat. Gillanders and Kingsford (2020) described the impacts of changes in the flow of freshwater on estuarine and open coastal habitats and admonished coastal environment managers to monitor these impacts. Monitoring the impacts can be challenging without the appropriate methods. Our paper presents the methods to facilitate such monitoring. Erosion and accretion of sediments can also account for Alternation. Alternation can sometimes derive from

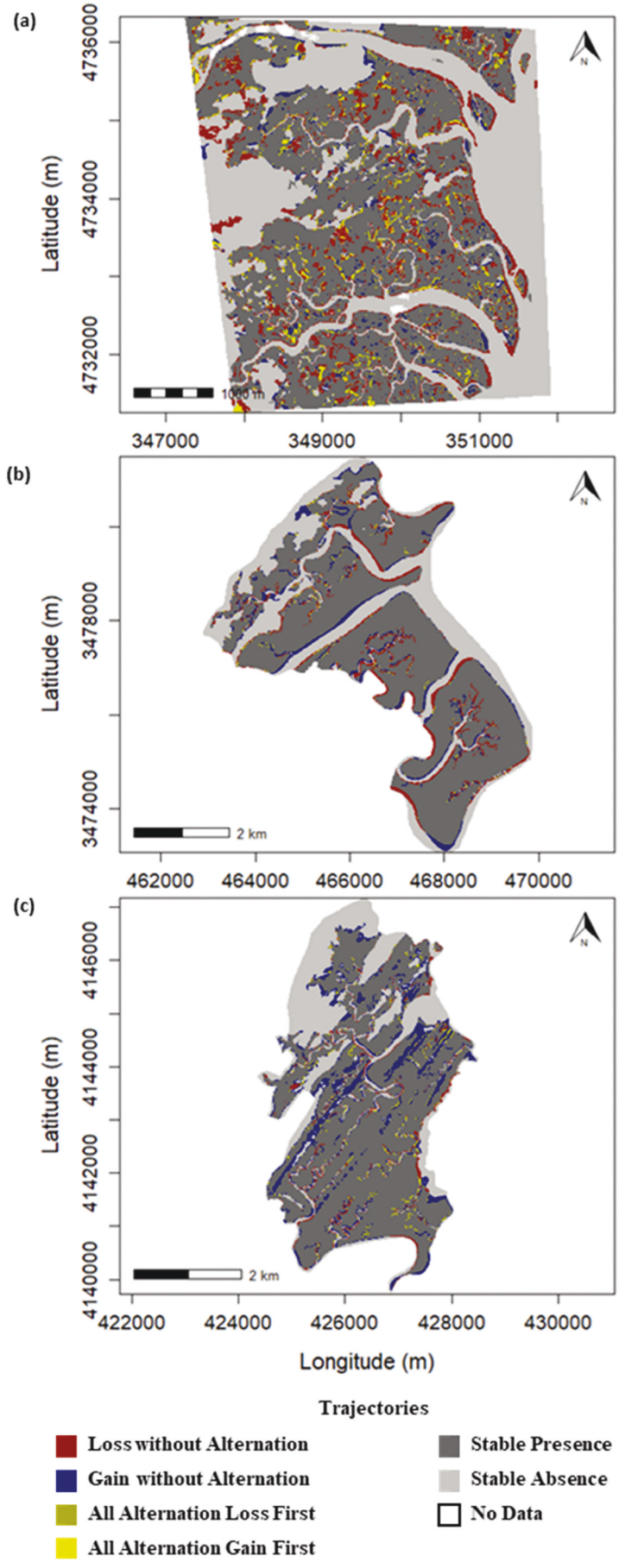

Figure 6. Trajectories for (a) PIE, (b) GCE, and (c) VCR.

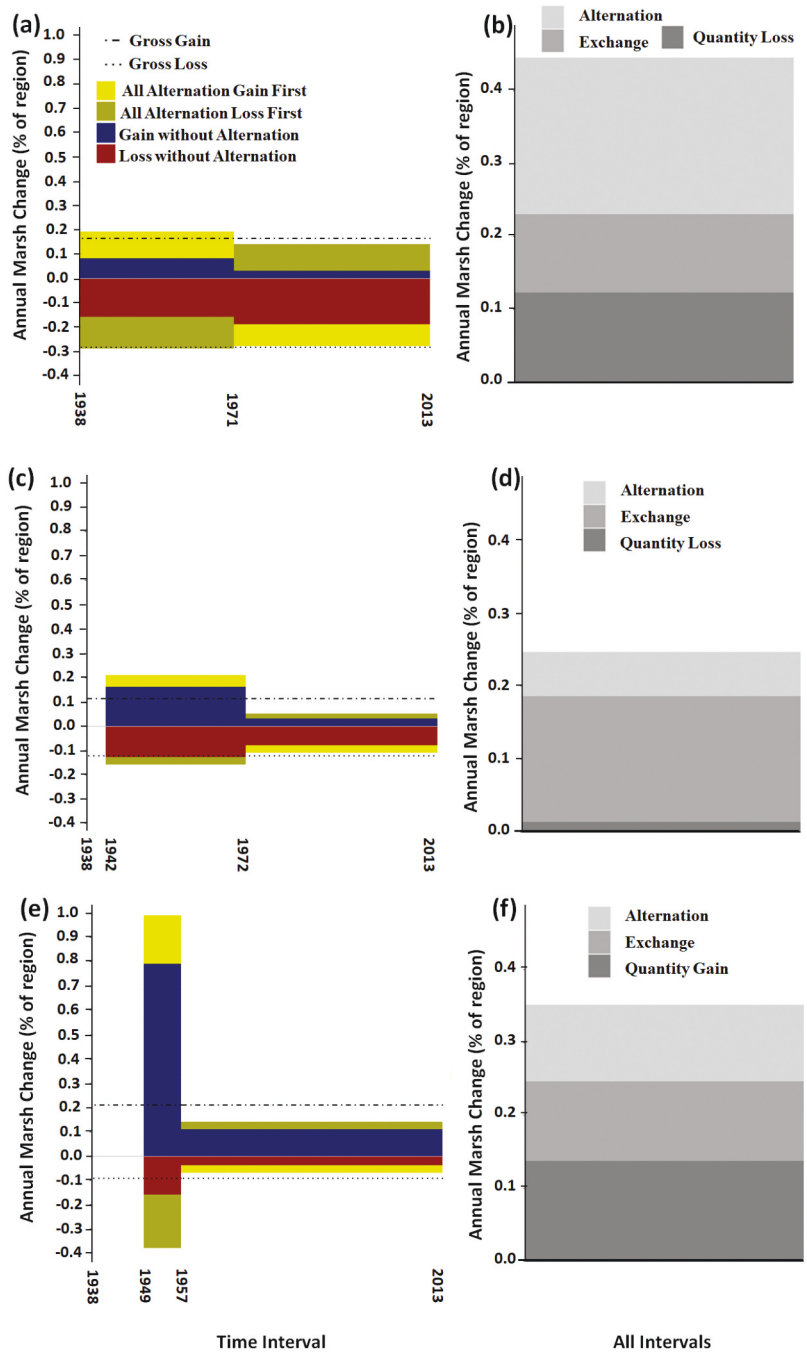

Figure 7. Marsh's trajectories of change in (a) PIE, (c) GCE, and (e) VCR during each time interval, and components of change in (b) PIE, (d) GCE, and (f) VCR.

poor data quality when analyzing a category such as urban, which is unlikely to alternate on the ground.

4.2. Denominators facilitate comparison across and within sites

Figure 6 shows that the sites vary in size of their spatial extents and marsh's prevalence in the extent at each time point. Equations 2 and 3 account for this variation by including each site's unified size in the denominator, facilitating comparison across sites. Furthermore, the years vary among the sites. Equations 4-5 and 7–8 have the duration of each site's temporal extent in the denominator, which facilitates comparison across sites. Equations 2 and 3 have each time interval's duration in the denominator, which facilitates comparison

across time intervals within each site. The denominators allow Figure 7 to express the vertical axis as the annual percentage of each site's unified size, which helps interpretation across sites. Our approach, therefore, avoids all the drawbacks of the three popular equations we described in the Introduction section (see Burns, Alber, and Alexander 2021; Liu et al. 2003; Puyravaud 2003).

Scientists tend to quantify land change by plotting the size of each land category as a function of time, which reveals net change during a time series (ICIMOD 2017; Kastens et al. 2017; MapBiomas n.d.; One Tree Planted n.d.; Padhee and Dutta 2019; Rosa et al. 2021). However, if a site experiences gross loss in some locations and gross gain in other locations during a time interval, then gross change is greater than absolute net change. For many sites, gross change is several times larger than absolute net change, in which case absolute net change misses most of the change.

The Quantity components in Figure 7 show that PIE experiences net loss of marsh, VCR experiences net gain of marsh, and GCE experiences close to zero net change, which is a function of only the size of marsh at start and end of the temporal extent. The Quantity component in our methodology shows the net change, including whether it is a net loss or net gain. However, our method goes deeper by evaluating trajectories of gross changes, which are impossible to see by considering only the size of marsh at each time point. For example, Figures 7a, c, and e show that gross change during the first time interval is greater than gross change during the second time interval for all sites, meaning change decelerates for all sites. Figures 7b, d, and f show that gross change during the temporal extent is fastest in PIE and slowest in GCE. The largest component in PIE is Alternation, in GCE is Exchange, and in VCR is Quantity. Quantity and Exchange derive from trajectories 1–4. Alternation derives from trajectories 3–6.

4.3. Interpretation must consider land change processes and data quality

Proper interpretation across sites requires an appreciation of the data's characteristics and knowledge of the land change processes (Pontius et al. 2018; Sertel, Robock, and Ormeci 2010; Washington-Ottombre et al. 2010). A coastal site's marsh can change by decade due to sea-level rise, by year due to sedimentation and erosion, by month due to seasonality, by week due to weather, and by hour due to tides (Burns, Alexander, and Alber 2020). Information availability dictated the data's years, which do not necessarily capture the temporal resolutions of the dynamics on the ground. Table 1 shows that the time points vary across winter, summer, and spring. We lack information concerning the precipitation in the days before the images and the tide level during the hour of the images. Therefore, it is unclear whether the variations across the three time points are due to changes on the ground across decade, year, season, day, or hour. Table 1 also shows how the images vary in terms of the technology that generated the images, which is likely to cause some of the maps' variation among the time points. Table 1 also reports the error in each map at each time point, which is typical for map producers to report. However, overall error does not give insight concerning errors for specific categories. Furthermore, errors at time points do not indicate the errors of change during the time intervals; therefore, it is unclear whether map errors could account for the differences between the time points.

4.4. Next steps

Our manuscript relies on pixel-by-pixel overlays of maps at various time points, thus capturing trajectories through time. However, this method does not capture spatial relationships because the method does not consider the patterns among neighboring pixels. Future publications will use the Total Operating Characteristic and multiple spatial resolutions to quantify the spatial relationships that the maps show. Visual inspection indicates that a substantial portion of the marsh's change is along the edge of the marsh, which makes sense as the marsh loses along its edge due to erosion and gains along the edge due to sedimentation. This indicates another potential flaw in the traditional equations that express a category's change during a time interval as a function of the category's size at the start of

the time interval. The marsh category is likely to change as a function of its edge length more than as a function of its size. Our future work will characterize the spatial relationship of change concerning distance to edge.

5. Conclusions

Our new methods quantify temporal change for a category to compare sites that vary in terms of spatial extent, temporal extent, temporal resolution, and the category's prevalence. The novel concept of Alternation quantifies the size of change that derives from gains and losses during sequential time intervals at the same location, while the unified size facilitates comparison across time intervals and among sites. The proposed methods quantify a category's change during a time series, as they facilitate cross-site comparison and provide more information than previous methods. We invite users to analyze the trajectories of a category during a time series by applying our *timeseriesTrajectories* R package, which is available for free at https://github.com/bilintoh/timeseriesTrajectories.

Acknowledgments

Clark Labs facilitated this work by creating the GIS software TerrSet®.

Disclosure statement

No potential conflict of interest was reported by the author(s).

Funding

The United States National Science Foundation's Division of Environmental Biology supported this work via grants OCE-1637630 and OCE-2224608 for the Plum Island Ecosystems Long-Term Ecological Research site. The United States National Aeronautics and Space Administration (NASA) also supported this work via the grant "Irrigation as climate-change adaptation in the Cerrado biome of Brazil evaluated with new quantitative methods, socio-economic analysis, and scenario models" Award # 80NSSC23K0508. The Humanize Institute supported this work via grant 21576 entitled "Methods and software to understand and build the MapBiomas data". The Edna Bailey Sussman Trust supplied additional funding.

ORCID

Thomas Mumuni Bilintoh http://orcid.org/0000-0002-6852-4439
Robert Gilmore Pontius Jr http://orcid.org/0000-0001-7287-5875
Aiyin Zhang http://orcid.org/0000-0001-6236-7105

Data and codes availability statement

The data that support the findings of this study are available at https://doi.org/10.6073/pasta/345165bcab691edd1f9ab6a92935f65b. The code that support the findings of this study is available at *https://github.com/bilintoh/timeseriesTrajectories*.

References

Aldwaik, S. Z., and R. G. Pontius. 2012. "Intensity Analysis to Unify Measurements of Size and Stationarity of Land Changes by Interval, Category, and Transition." *Landscape and Urban Planning* 106 (1): 103–114. https://doi.org/10.1016/j.landurbplan.2012.02.010.

Borrelli, P., D. A. Robinson, P. Panagos, E. Lugato, J. E. Yang, C. Alewell, and C. Ballabio. 2020. "Land Use and Climate Change Impacts on Global Soil Erosion by Water (2015-2070)." *Proceedings of the National Academy of Sciences of the United States of America* 117 (36): 21994–22001. https://doi.org/10.1073/pnas.2001403117.

Burns, C. J., M. Alber, and C. R. Alexander. 2021. "Historical Changes in the Vegetated Area of Salt Marshes." *Estuaries & Coasts* 44 (1): 162–177. https://doi.org/10.1007/s12237-020-00781-6.

Burns, C. J., C. R. Alexander, and M. Alber. 2020. "Assessing Long-Term Trends in Lateral Salt-Marsh Shoreline Change Along a U. S. East Coast Latitudinal Gradient." *Journal of Coastal Research* 37 (2): 291–301. https://doi.org/10.2112/JCOASTRES-D-19-00043.1.

Burns, C. 2020. *Cross-site comparison of historical trends in marsh change at three LTER sites: GCE, VCR, and PIE*. [Dataset]. Environmental Data Initiative. https://doi.org/10.6073/PASTA/345165BCAB691EDD1F9AB6A92935F65B.

Campbell, A. D., L. Fatoyinbo, L. Goldberg, and D. Lagomasino. 2022. "Global Hotspots of Salt Marsh Change and Carbon Emissions." *Nature* 612:701–708. https://doi.org/10.1038/s41586-022-05355-z.

Chowdhury, S., D. K. Chao, T. C. Shipman, and M. A. Wulder. 2017. "Utilization of Landsat Data to Quantify Land-Use and Land-Cover Changes Related to Oil and Gas Activities in West-Central Alberta from 2005 to 2013." *GIScience & Remote Sensing* 54 (5): 700–720. https://doi.org/10.1080/15481603.2017.1317453.

Clement, F., and J. M. Amezaga. 2008. "Linking Reforestation Policies with Land Use Change in Northern Vietnam: Why Local Factors Matter." *Geoforum* 39 (1): 265–277. https://doi.org/10.1016/j.geoforum.2007.05.008.

Dasgupta, S., B. Laplante, C. Meisner, D. Wheeler, and J. Yan. 2009. "The Impact of Sea Level Rise on Developing Countries: A Comparative Analysis." *Climatic Change* 93 (3–4): 379–388. https://doi.org/10.1007/s10584-008-9499-5.

Fagherazzi, S., G. Mariotti, N. Leonardi, A. Canestrelli, W. Nardin, and W. S. Kearney. 2020. "Salt Marsh Dynamics in a Period of Accelerated Sea Level Rise." *Journal of Geophysical Research: Earth Surface* 125 (8): 1–31. https://doi.org/10.1029/2019JF005200.

FAO & JRC. 2012. "Global Forest Land-Use Change 1990–2005." *FAO Forestry Paper No. 169*. http://www.fao.org/docrep/017/i3110e/i3110e.pdf. In Fao.

Feng, Y., and X. Tong. 2018. "Dynamic Land Use Change Simulation Using Cellular Automata with Spatially Nonstationary Transition Rules." *GIScience & Remote Sensing* 55 (5): 678–698. https://doi.org/10.1080/15481603.2018.1426262.

Gillanders, B. M., and M. Kingsford. 2020. "Impact of Changes in Flow of Freshwater on Estuarine and Open Coastal Habitats and the Associated Organisms." *Oceanography and Marine Biology* 40:233–309.

Grekousis, G., G. Mountrakis, and M. Kavouras. 2016. "Linking MODIS-Derived Forest and Cropland Land Cover 2011 Estimations to Socioeconomic and Environmental Indicators for the European Union's 28 Countries." *GIScience & Remote Sensing* 53 (1): 122–146. https://doi.org/10.1080/15481603.2015.1118977.

Heintzman, L. J., N. E. Mcintyre, E. J. Langendoen, and Q. D. Read. 2024. "Cultivation and Dynamic Cropping Processes Impart Land - Cover Heterogeneity within Agroecosystems: A Metrics - Based Case Study in the Yazoo - Mississippi Delta." *Landscape Ecology* 39 (29): 1–29. https://doi.org/10.1007/s10980-024-01797-0.

ICIMOD. 2017. "Regional Land Cover Monitoring System. https://geoapps.icimod.org/rlcms.

Kastens, J. H., J. C. Brown, A. C. Coutinho, C. R. Bishop, and J. C. D. M. Esquerdo. 2017. "Soy Moratorium Impacts on Soybean and Deforestation Dynamics in Mato Grosso, Brazil." *PLoS One* 12 (4): 1–21. https://doi.org/10.1371/journal.pone.0176168.

Liu, J., M. Liu, D. Zhuang, Z. Zhang, and X. Deng. 2003. "Study on Spatial Pattern of Land-Use Change in China During 1995-2000." *Science in China Series D: Earth Sciences* 46 (4): 373384. https://doi.org/10.1360/03yd9033.

Lopes, C. L., R. Mendes, I. Caçador, and J. M. Dias. 2020. "Assessing Salt Marsh Extent and Condition Changes with 35 Years of Landsat Imagery: Tagus Estuary Case Study." *Remote Sensing of Environment* 247 (April): 14. https://doi.org/10.1016/j.rse.2020.111939.

MapBiomas. n.d. Plataforma-MapBiomas Brasil. Accessed October 19, 2022 https://mapbiomas.org/.

Molotoks, A., P. Smith, and T. P. Dawson. 2021. "Impacts of Land Use, Population, and Climate Change on Global Food Security." *Food and Energy Security* 10 (1): 1–20. https://doi.org/10.1002/fes3.261.

One Tree Planted. n.d. "Global Forest Watch." Accessed October 19, 2022, from 2014 website. https://www.globalforestwatch.org/dashboards/global/.

Padhee, S. K., and S. Dutta. 2019. "Spatio-Temporal Reconstruction of MODIS NDVI by Regional Land Surface Phenology and Harmonic Analysis of Time-Series." *GIScience & Remote Sensing* 56 (8): 1261–1288. https://doi.org/10.1080/15481603.2019.1646977.

Pontius, R. G., J.-C. Castella, T. de Nijs, Z. Duan, E. Fotsing, N. Goldstein, and A. T. Veldkamp. 2018. "Lessons and Challenges in Land Change Modeling Derived from Synthesis of Cross-Case Comparisons." *Trends in Spatial Analysis and Modelling Geotechnologies and the Environment*: 143–164. https://doi.org/10.1007/978-3-319-52522-8_8.

Pontius, R. G., J. Huang, W. Jiang, S. Khallaghi, Y. Lin, J. Liu, and S. Ye. 2017. "Rules to Write Mathematics to Clarify Metrics Such as the Land Use Dynamic Degrees." *Landscape Ecology* 32 (12): 2249–2260. https://doi.org/10.1007/s10980-017-0584-x.

Pontius, R. G., R. Krithivasan, L. Sauls, Y. Yan, and Y. Zhang. 2017. "Methods to Summarize Change Among Land Categories Across Time Intervals." *Journal of Land Use Science* 12 (4): 218–230. https://doi.org/10.1080/1747423X.2017.1338768.

Pontius, R. G., and M. Millones. 2011. "Death to Kappa: Birth of Quantity Disagreement and Allocation Disagreement for Accuracy Assessment." *International Journal of Remote Sensing* 32 (15): 4407–4429. https://doi.org/10.1080/01431161.2011.552923.

Pontius, R. G., and A. Santacruz. 2014. "Quantity, Exchange, and Shift Components of Difference in a Square Contingency Table." *International Journal of Remote Sensing* 35 (21): 7543–7554. https://doi.org/10.1080/2150704X.2014.969814.

Puyravaud, J. P. 2003. "Standardizing the Calculation of the Annual Rate of Deforestation." *Forest Ecology & Management* 177 (1–3): 593–596. https://doi.org/10.1016/S0378-1127(02)00335-3.

Rosa, M. R., P. H. S. Brancalion, R. Crouzeilles, L. R. Tambosi, P. R. Piffer, F. E. B. Lenti, and J. P. Metzger. 2021. "Hidden Destruction of Older Forests Threatens Brazil's Atlantic Forest and Challenges Restoration Programs." *Science Advances* 7 (4): 1–8. https://doi.org/10.1126/sciadv.abc4547.

Roy, M. S., J. E. K. Byrnes, and G. Mavrommati. 2024. "Mitigation Policies Buffer Multiple Climate Stressors in a Socio-Ecological Salt Marsh Habitat." *Sustainability Science* 19 (1): 245–258. https://doi.org/10.1007/s11625-023-01414-0.

Ruskule, A., O. Nikodemus, Z. Kasparinska, R. Kasparinskis, and G. Brūmelis. 2012. "Patterns of Afforestation on Abandoned

Agriculture Land in Latvia." *Agroforestry Systems* 85 (2): 215–231. https://doi.org/10.1007/s10457-012-9495-7.

Sertel, E., A. Robock, and C. Ormeci. 2010. "Impacts of Land Cover Data Quality on Regional Climate Simulations." *International Journal of Climatology* 30 (13): 1942–1953. https://doi.org/10.1002/joc.2036.

Taubert, F., R. Fischer, J. Groeneveld, S. Lehmann, M. S. Müller, E. Rödig, and A. Huth. 2018. "Global Patterns of Tropical Forest Fragmentation." *Nature* 554 (7693): 519–522. https://doi.org/10.1038/nature25508.

Washington-Ottombre, C., B. Pijanowski, D. Campbell, J. Olson, J. Maitima, A. Musili, and A. Mwangi. 2010. "Using a Role-Playing Game to Inform the Development of Land-Use Models for the Study of a Complex Socio-Ecological System." *Agricultural Systems* 103 (3): 117–126. https://doi.org/10.1016/j.agsy.2009.10.002.

Winkler, K., R. Fuchs, M. Rounsevell, and M. Herold. 2021. "Global Land Use Changes are Four Times Greater Than Previously Estimated." *Nature Communications* 12 (1): 1–10. https://doi.org/10.1038/s41467-021-22702-2.

Zomer, R. J., A. Trabucco, D. A. Bossio, and L. V. Verchot. 2008. "Climate Change Mitigation: A Spatial Analysis of Global Land Suitability for Clean Development Mechanism Afforestation and Reforestation." *Agriculture, Ecosystems & Environment* 126 (1–2): 67–80. https://doi.org/10.1016/j.agee.2008.01.014.